Soft Origami: Classification, Constraint, and Actuation of Highly Compliant Origami Structures

Charles M. Wheeler
Massachusetts Institute of Technology,
77 Massachusetts Avenue,
35-135,
Cambridge, MA 02139
e-mail: wheelerc@mit.edu

Martin L. Culpepper
Fellow ASME
Massachusetts Institute of Technology,
77 Massachusetts Avenue,
35-237,
Cambridge, MA 02139
e-mail: culpepper@mit.edu

Herein, we discuss the folding of highly compliant origami structures—"Soft Origami." There are benefits to be had in folding compliant sheets (which cannot self-guide their motion) rather than conventional rigid origami. Example applications include scaffolds for artificial tissue generation and foldable substrates for flexible electronic assemblies. Highly compliant origami has not been contemplated by existing theory, which treats origami structures largely as rigid or semirigid mechanisms with compliant hinges—"mechanism-reliant origami." We present a quantitative metric—the origami compliance metric (OCM)—that aids in identifying proper modeling of a homogeneous origami structure based upon the compliance regime it falls into (soft, hybrid, or mechanism-reliant). We discuss the unique properties, applications, and design drivers for practical implementation of Soft Origami. We detail a theory of proper constraint by which an ideal soft structure's number of degrees-of-freedom may be approximated as 3n, where n *is the number of vertices of the fold pattern. Buckling and sagging behaviors in very compliant structures can be counteracted with the application of tension; we present a method for calculating the tension force required to reduce sagging error below a user-prescribed value. Finally, we introduce a concept for a scalable process in which a few actuators and stretching membranes may be used to simultaneously fold many origami substructures that share common degrees-of-freedom.* [DOI: 10.1115/1.4032472]

Introduction

Soft Origami is relevant to modern engineering due to an increased need to form components and assemblies from highly compliant substrates. There are many applications where existing technology could be used to create intricate 2D patterns that, if transformed into a 3D geometry, would be enabled. For example, flexible electronics may be made with existing 2D processes, but could then be folded into 3D patterns to achieve smaller, more space-efficient packages [1].

There is also the potential to create 2D patterns for tissue scaffolding (including vasculature, connective tissues, nerves, etc.), deposit cells, and then fold the scaffolds to yield suitable 3D geometries. Successful production of viable, correctly functioning organs requires not only the presence of the appropriate cell types but also the ability to correctly arrange cells in relation to one another in 3D space [2–5]. Existing approaches remain limited in two ways: parallel, high-throughput methods lack the capability to achieve complex 3D microstructures [6–9]; and serial, high-accuracy, fine-resolution methods (such as 3D printing) remain expensive and rate-limited [10,11]. Origami-inspired assembly of tissue scaffolds by folding of cell-seeded sheets is one approach with the potential to achieve high-throughput and high spatial complexity at low-cost.

The bulk of existing analysis and design theory considers an origami structure to be a network of rigid or semirigid panels interconnected by compliant hinges [12–14]. Panels provide stiffness, structure, and self-constraint, while hinges introduce folding degrees-of-freedom, thus yielding a mechanismlike behavior. It is common to depict origami using conjugate hinge-linkage mechanisms—the spherical mechanism, an analog to the four-hinge vertex found in many patterns such as the Miura-ori, is one popular example [15].

The practical implementation of these mechanismlike assemblies relies upon distinct "panel" and "hinge" features within the origami structure. The difference in function between these elements—panels providing stiffness and hinges providing compliance—manifests in the form of dedicated componentry (bushings, bearings) or geometric design features at the hinges, such as the living hinges as shown in Fig. 1.

The production of large assemblies with many small-scale elements or features (potentially micro- and nanoscale) would require hundreds or thousands of panels and hinges. Practical implementation requires a different approach.

We are investigating Soft Origami as one potential solution. Soft Origami structures are composed of complaint sheets that are capable of localized bending and creasing. An analogy may be

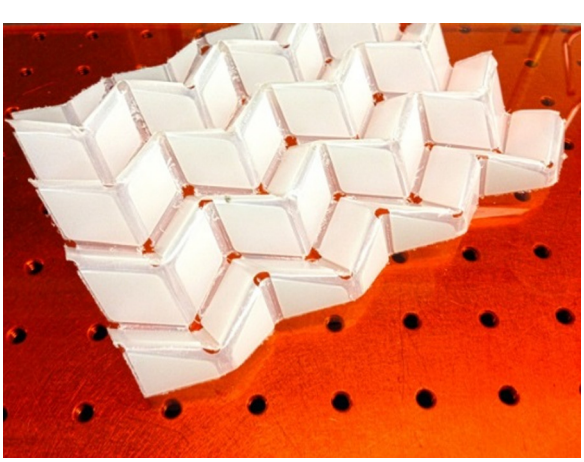

Fig. 1 Miura-ori lattice machined from high-density polyethylene (HDPE). Bending allowed by living hinges, this structure's designed-in mechanism feature.

Manuscript received September 14, 2015; final manuscript received December 17, 2015; published online May 4, 2016. Assoc. Editor: James Schmiedeler.

made to bedsheets, which do not have dedicated hinges or folding components, but instead rely on the user to impose folds and dictate the system's final geometry. Soft Origami structures exhibit similarly high levels of compliance (a metric we quantify later on) and no dedicated hinge features are needed; external constraints guide the structure into the right geometry.

We begin by presenting a quantitative metric for identifying sheet materials and geometries that may be folded within this framework. We discuss the characteristic behavior for each of three compliance regimes—soft, hybrid, and mechanismlike. We discuss the constraint of Soft Origami, demonstrating that for best performance, a structure should always be held in tension. We discuss the approximation of degrees-of-freedom relative to the number of vertices within an origami pattern. Finally, we close by introducing a concept which uses prestrained membranes as a means for actuating Soft Origami structures.

Definitions

Hinge—A designed-in feature allowing for the folding of an origami structure. A hinge is an engineering term that describes the physical embodiment of a crease line on an origami fold pattern. Each possesses finite thickness, length, width, and material properties.

Lattice—The origami structure to be folded, including any designed-in hinges or panels.

Membranes—The elastic sheets proposed as potential actuators for driving folding of Soft Origami structures.

Panel—A panel is an engineering term that describes the physical embodiment of a facet on an origami fold pattern. Each possesses finite thickness, length, width, and material properties. Although intended to remain planar during and after folding, a panel may exhibit nonideal behaviors such as bending and buckling. Each panel is bordered by hinges and/or the edges of the folding sheet.

OCM and Regimes

Qualitative Behavior of Soft Origami. Later in this paper, we present a quantitative definition for Soft Origami, but first it is important to establish *qualitative* intuition for how it behaves. At a high level, origami-inspired folding entails: the demarcation of a two-dimensional surface into distinct conjoined regions (shapes); and, the reorientation of these shapes through actuation to produce a new and distinct two- or three-dimensional topology. Origami may be externally or internally actuated [16–25], but historically has been designed to be self-constraining (panel and hinge rigidities and pattern layout dictate its degrees-of-freedom). In other words, conventional origami is internally guided and internally or externally actuated. Soft Origami differs in which it must be both externally guided and externally actuated.

An *idealized* Soft Origami structure is considered to be perfectly *pliant*. It may bend (and to a limited extent, stretch), as shown in Fig. 2, to any imposed curvature. This compliant behavior means that an ideal Soft Origami structure has no capability to support itself under compressive loads such as gravity—its degrees-of-freedom are fixed only through connection with its external constraints. A sheet may be directed into a variety of desired topologies without the need for dedicated hinge or panel features.

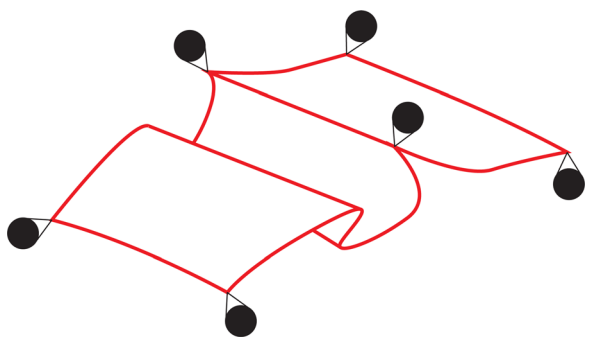

Fig. 2 Illustration of ideal Soft Origami sheet, capable of bending to any curvature

It is important to establish a quantitative metric for classifying a given origami structure's relative compliance. Such a metric may be used by a designer to quickly identify and predict Soft Origamilike behavior to tune a folding system for more desirable Soft Origami characteristics, or to validate the use of Soft Origami assumptions presented herein. Alternatively, it may be used to examine a hinged system's fitness to rigid-origami assumptions.

Important Criteria for a Compliance Metric. We considered the following criteria when formulating this compliance metric:

- Geometry: The geometry of a single representative panel from the selected origami lattice.
- Material: The compliance and failure limits depend on the material from which the lattice is constructed.
- Large Deflections: By its nature, origami involves large deflections; our metric considers a load case that has a straightforward large deflection solution (note that large deflections do not imply large local material deformations—they must still be small in this model).
- Deformed Shape: Our metric concerns the maximum deflection a panel may achieve. We therefore apply a *displacement condition* and impose uniform curvature upon the panel to replicate the case of greatest possible deflection before failure.

Assumptions

(1) The sheet to be folded is of uniform thickness, is continuous, and all panels in the origami fold pattern are identical (the OCM is the same for all panels).
(2) The thickness of the sheet to be folded is such that the continuum limit is not reached and the origami lattice may be considered a *continuum* at all locations:
  (a) It is infinitely divisible.
  (b) It is locally homogeneous (material properties do not change, even if the structure is subdivided many times).
(3) The origami lattice is composed of an idealized isotropic, linear-elastic material.
(4) The origami lattice material exhibits a well-defined Young's modulus (E) and failure strength (σ_f).
(5) Although the total tip-to-tip *deflection* of the structure may be large, local *deformations* are small and anticlastic deformations (those within the cross section of the panel) may be ignored. As discussed later, this holds true so long as the radius of curvature in bending (ρ) is large when compared to the thickness of the structure $(\rho/t > 10)$ [26].

Derivation of the OCM. Being perfectly compliant, an ideal Soft Origami panel may deform to any curvature. Perhaps the simplest and most versatile approximation of a panel—a rectangular prismatic beam of relatively great width—approaches this ideal case when its radius of curvature at first failure becomes very small in comparison with its length.

We begin our derivation by extracting a representative panel from the lattice of interest and modeling it as a wide beam. We consider the shortest edge of the panel, as this will produce the most conservative compliance estimate. We then impose a uniform curvature on the beam through the use of a moment loading, as shown in Fig. 3.

In practice, each origami system will experience 3D loading involving multiple moments and forces from adjacent panels. This

metric is not intended to model the panel's precise reaction to this type of loading condition. Rather, it provides an *assessment of the greatest total deflection the panel could conceivably achieve at the instant before failure*. The moment loading is therefore only used as a mathematical tool to achieve the constant-curvature displacement condition.

In this scenario, the curvature along the length of the beam is uniform and the displacement solution for this case is valid even for large displacements. The classic moment-curvature relation for this wide beam is [27]

$$\kappa = \frac{M(1-\nu^2)}{\mathrm{EI}} \tag{1}$$

where M is imposed moment, E is Young's modulus, I is bending moment of inertia, κ is beam curvature, and ν is Poisson's ratio.

As with curvature, the stress distribution in the beam remains constant along its length, varying only with distance from the beam's neutral axis

$$\sigma_b = \frac{\mathrm{Mz}}{I} \tag{2}$$

where σ_b is the bending stress and z is the distance from neutral axis

Expressed in terms of the beam's curvature

$$\sigma_b = \frac{\mathrm{E}\kappa\mathrm{z}}{1-\nu^2} \tag{3}$$

A beam in pure bending may be said to fail when the maximum bending stress exceeds the material's failure stress (σ_f). In selecting a failure stress, Ashby recommends choosing the yield strength for metals and polymers, the modulus of rupture for ceramics, the tear strength for elastomers, and the tensile strength for composites and woods [28]. Recalling the assumptions of an isotropic, linear-elastic material with well-defined Young's modulus, we remind the reader that the predictive power of this estimate will lessen as a material strays from these assumptions.

The curvature at which peak bending stress occurs—the maximum attainable curvature for the beam before failure—is

$$\kappa = \frac{2\sigma_f(1-\nu^2)}{\mathrm{Et}} \tag{4}$$

Here, t is the beam thickness. The total angle through which the beam curves from tip-to-tip is

$$\theta = \kappa \mathrm{L} \tag{5}$$

For an idealized origami mechanism, the terminal folding angle is 180 deg, at which point the panels adjacent to the fold meet; we assign θ a value of π radians, and so the minimum length needed for a beam to bend 180 deg without failure is

$$L_{180} = \frac{\pi E t}{2\sigma_f(1-\nu^2)} \tag{6}$$

L_{180} represents the minimum panel length necessary to achieve a full 180 deg bend before inducing material failure. If a panel has thickness, t, Young's modulus, E, failure strength, σ_f, and is significantly longer than L_{180}, the panel is capable of achieving large curvatures without failure. Likewise, a panel with identical thickness and material properties but length significantly smaller than L_{180} will be unable to achieve such large bending deflections without failing. The OCM—our metric for quantifying an origami structure's capacity to deform—is expressed as

$$\mathrm{OCM} = \frac{L_{180}}{L} = \frac{\pi}{2}\frac{t}{L}\frac{E}{\sigma_f}\left(\frac{1}{1-\nu^2}\right) \tag{7}$$

Or, in terms of the minimum radius of curvature at failure (ρ_{180}), where $\rho_{180} = L_{180}/\pi$

$$\mathrm{OCM} = \frac{\pi\rho_{180}}{L} \tag{8}$$

OCM Regimes. An ideal Soft Origami structure may achieve an infinitely small bending radius; its OCM is identically zero. For engineering and design purposes, we designate three behavioral modes with respect to the OCM as seen in Fig. 4.

- Soft Origami (OCM $\ll$ 1): The lattice is capable of extreme deflections without hinges. It will readily conform to displacements imposed by external constraints and actuators. The lattice degrees-of-freedom are externally defined by its actuators.
- Mechanism-reliant origami (OCM $\gg$ 1): The lattice requires hinges to achieve large deflections. Imposing large deflections without hinges will result in material damage and/or failure. The lattice degrees-of-freedom are internally defined by its geometry and panel stiffness.
- Hybrid origami (OCM $\approx$ 1): The lattice is capable of moderately large deflections before failure, but a significant fraction of the panel must bend to accommodate such deflections. The lattice will not readily conform to arbitrary

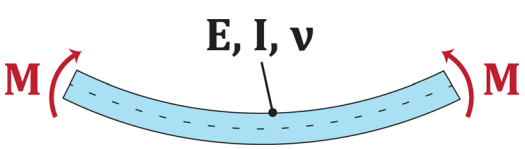

Fig. 3 Model of wide beam exposed to moment loads "M." The beam exhibits constant curvature along its length

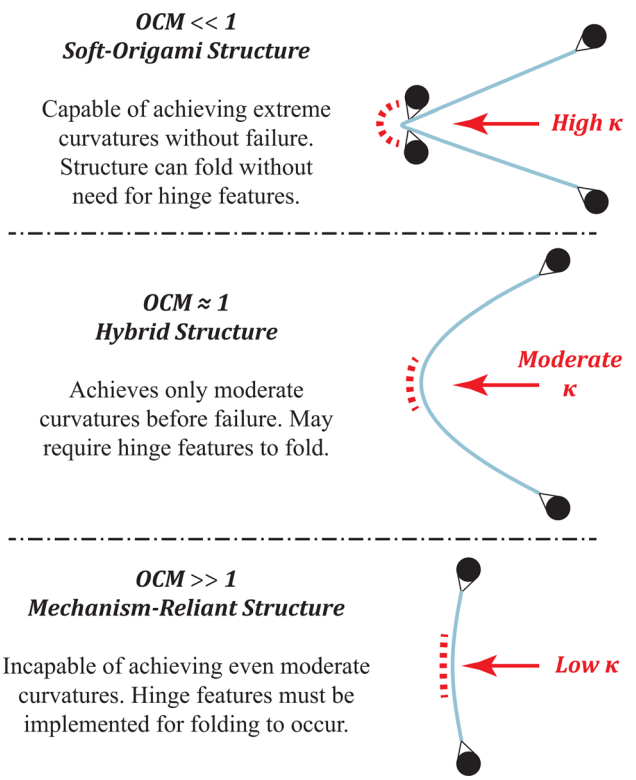

Fig. 4 Examples of peak curvatures achievable by structures representing each of the three OCM regimes

geometries. The lattice degrees-of-freedom depend on both its external actuators and its own geometry/stiffness (it is not exclusively internally or exclusively externally defined).

When evaluating a system using this metric, it is important to remember that the OCM value is not a measure of the structure's *resistance to deflection under load*; it is not a stiffness estimate. Rather, it is a measure of the structure's *capacity to achieve large deflections without failing*.

OCM Examples. In Table 1, we give two OCM values to provide an intuitive example of what the OCM value means; plastic wrap and sheet metal serve as familiar examples. Often to the frustration of the user, plastic wrap used for storing food seems capable of assuming virtually any shape and it falls well within the Soft Origami regime. By comparison, a 1.5-mm thick steel square would be classified as a mechanism-reliant structure because it must experience significant yielding before even moderate deflections would occur.

Design Factors for Tuning an Assembly's OCM Value. An engineer interested in tuning the OCM of an origami system may do so by adjusting the system's material properties and geometry. The relationship between the OCM and the tunable property is proportional to first order in both cases

$$\text{OCM} \propto t/L \tag{9}$$

$$\text{OCM} \propto E/\sigma_f \tag{10}$$

Origami designs are typically specified with prescribed panel shapes and lengths, so adjustment of the OCM value by geometry is most easily accomplished by changing the thickness of the folding substrate. Panel thickness values are generally dictated by material processing limitations and design requirements of the system, though thickness changes of 1–2 orders of magnitude are feasible in some cases.

The OCM varies by roughly 3 orders of magnitude for different engineering materials, with the ratio E/σ_f ranging from a minimum of roughly ~ 10 (plastics and polymers) to a maximum of $\sim 10,000$ (some metals and ceramics). Performance may therefore be changed drastically by simply selecting a different material for folding.

In the limiting case where both the geometric and material ratios range from their extreme values, the OCM value may vary by a factor of $\sim 100,000$. In practice, where the range of valid materials and geometries is more limited, a more feasible expectation for adjustment of the OCM value is a factor of $\sim 100 - \sim 1000$.

Extension to Nonuniform Origami Sheets. A lattice exhibiting nonuniformities in thickness, in panel dimensions, or in material properties may not exhibit a constant OCM across its entire structure. In this case, the full range of OCM values for the lattice must be considered. Calculating the OCM across all panels allows one to produce a map of the compliance behavior across the structure, while calculating the OCM for the least- and most-compliant panels will produce the range of values under which the lattice will behave. Even if some or many values differ, if all values are contained within a single compliance regime, the lattice as a whole may be said to behave within that regime (it will be globally soft, hybrid, or mechanism-reliant). If the OCM values span multiple regimes, the lattice will exhibit locally soft, hybrid, or mechanism-reliant behavior but global classification for the entire structure is not possible.

Table 1 Example OCM values for two 25 mm × 25 mm panels

	Plastic wrap (HDPE)	Sheet metal (1018 Steel)
E (GPa)	1	205
t (mm)	0.0125	1.5
σ_f (MPa)	20	250
L (mm)	25	25
ν	0.40	0.29
OCM	0.047	84

Limitations. The fifth assumption in this model—negligible anticlastic deformations—assumes the local radius of curvature is large in comparison with the thickness of the material. In this analysis, the radius of curvature/thickness ratio may be written as

$$\frac{\rho_{180}}{t} = \frac{E}{2\sigma_f} \tag{11}$$

For most engineering materials, the ratio of Young's modulus (E) to failure stress (σ_f) is at least 10:1; for metals and many plastics and polymers, the ratio is approaches or exceeds 100:1 [6]. In the case of these materials, the approximation presented will serve as a good estimate of the material's response to an induced deflection. However, many elastomers exhibit ratios less than 1:1 and the designer should proceed with caution.

Constraint of Soft Origami Structures

Rayleigh–Ritz Buckling Criterion. Ideal Soft Origami structures cannot support compressive loads and must be constrained externally. This is easily demonstrated using the Rayleigh–Ritz buckling quotient resulting from the principle of virtual work. For a beam of relatively great width, the net critical compressive load needed to induce buckling is [29]

$$N = \frac{\text{EI}}{1-\nu^2} \frac{\int_0^L \delta \text{w}'' \delta \text{w}'' dx}{\int_0^L \delta \text{w}' \delta \text{w}' dx} \tag{12}$$

where N is critical buckling load, E is Young's modulus, I is the bending moment of inertia, L is the beam length, and ν is Poisson's ratio.

In this formulation, w is the characteristic shape function associated with deflection during buckling. The variables $\delta w'$ and $\delta w''$ are the first and second variations of the shape function, respectively.

The zero-thickness assumption for an ideal Soft Origami structure produces a zero-valued moment of inertia (I) and therefore a zero-valued critical buckling load; the structure will buckle under any imposed compressive load.

Tension to Prevent Buckling and Sagging. As demonstrated, ideal Soft Origami cannot sustain a *net* compressive load, but induced tensile forces are tolerable and will work to prevent buckling. This result has important practical implications: to avoid buckling failure in a functional Soft Origami device (which experiences loads such as gravity), one must maintain a net tension in each in-plane direction across all points on all faces. This could be accomplished (though perhaps not in the most practical way) by assigning an actuator to each vertex and then maintaining a tension force between all adjacent actuator pairs (each pair of vertices connected by a single edge on the folding diagram).

Sagging of the panel due to gravity is also counteracted by imposing tension. An upper bound for the tension needed to acceptably counteract sagging can be derived by assuming a worst-case scenario where: (a) the panel is positioned horizontally (gravity acts transversely) and (b) the panel behaves as ideal Soft Origami (it has zero bending stiffness). Making these assumptions, a Soft Origami panel behaves as a level-span catenary

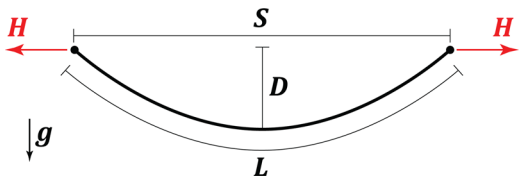

Fig. 5 The level-span catenary suspension representation of sagging panel. Note that vertical forces (not pictured here) are also exerted at the endpoints of the span, with total magnitude equivalent to the weight of the span.

element, as shown in Fig. 5. We seek an expression for the horizontal tension force (relative to the weight of the panel) required to reduce sagging below a desired level; this relationship is derived here.

We begin with the two well-known equations governing a standard catenary element

$$D = \frac{H\left(\cos h\left(\frac{Sw}{2H}\right) - 1\right)}{w} \tag{13}$$

$$L = \frac{(2H)\sin h\left(\frac{Sw}{2H}\right)}{w} \tag{14}$$

where S is the spanned length, D is the sag height, w is the panel weight per unit length, L is panel length, H is horizontal tension force, and g is direction of gravity.

We define the horizontal tension force to be a multiple, c, of the total panel weight

$$c = \frac{H}{Lw} \tag{15}$$

where c is the tension ratio (horizontal tension to total span weight).

Solving for the suspension length, L, needed to span S with a tension ratio c

$$L = \frac{S}{(2c)\sin h^{-1}\left(\frac{1}{2c}\right)} \tag{16}$$

The nondimensional ratio of sag height to the spanned length, D/S, as a function of tension ratio c, can therefore be expressed as

$$\frac{D}{S} = \frac{\sqrt{\frac{1}{4c^2} + 1} - 1}{2\mathrm{csch}^{-1}(2c)} \tag{17}$$

The sagging ratio is highly sensitive to the horizontal tension ratio, as seen on the log–log plot in Fig. 6.

As the tension ratio reaches $c = 10$ (where the horizontal tension force is ten times the weight of the panel), the sagging ratio is approximately $D/S = 0.0125$. We therefore recommend a tension ratio of $c = 10$ or greater in order to reduce sag error below 1.25% (sagging is further reduced by panel stiffness and increasingly vertical orientation).

Degrees-of-Freedom. For a folding pattern with n vertices, we assign n actuators. As each vertex has three translational degrees-of-freedom in Cartesian space, an ideal Soft Origami structure—with zero-thickness, zero weight, and zero minimum bending radius—therefore can be idealized to have $3n$ degrees-of-freedom. This assumes there are no rotational degrees-of-freedom associated with the vertices.

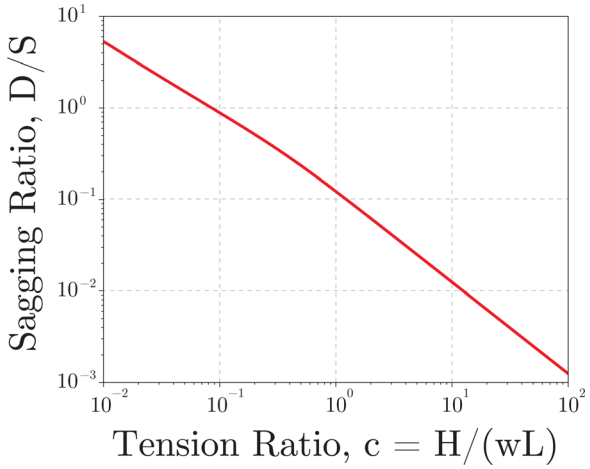

Fig. 6 Sagging ratio as a function of tension ratio

We may use this result to approximate a nonideal structure's degrees-of-freedom as also being $3n$; this approximation becomes more accurate with decreasing OCM values, decreasing contact area at the actuator–lattice interface, and increasing the imposed tensions (this will reduce sagging deflections induced by gravity).

Actuation of Soft Origami Structures

Any actuation mechanism for folding Soft Origami must satisfy many functional requirements. An ideal actuation mechanism must:

- Constrain and actuate each vertex
- Avoid interference between actuators/actuation points
- Simultaneously actuate all vertices along precise paths
- Achieve large actuation strokes relative to the lattice size
- Possess great stiffness relative to that of the folding lattice
- Avoid any self-interference
- Robustly scale with the number of vertices
- Robustly scale with the characteristic panel size

Of these, robust scaling with respect to vertex count is perhaps the most difficult requirement. This is because, for a square grid of vertices, the total vertex count scales as n^2, where n is the vertex count on an edge. Folding of very small Soft Origami assemblies is straightforward, as an independent, dedicated actuator can be assigned to each vertex. This approach loses feasibility as the size of the origami lattice increases. For example, the lattice depicted in Fig. 7—measuring just six panels by six panels—

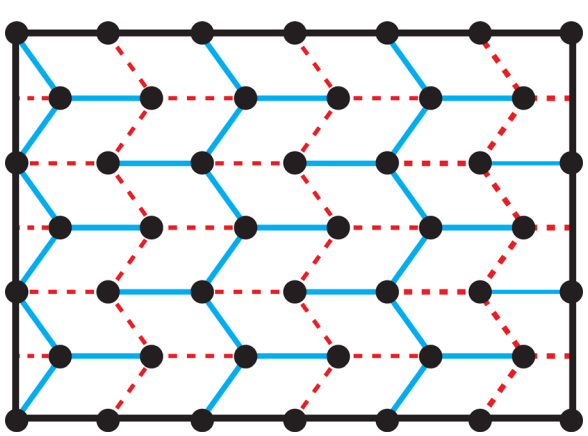

Fig. 7 6 × 6-panel Miura-ori folding diagram. Dotted lines, solid interal lines, and dots represent valley folds, mountain folds, and vertices, respectively.

would already require nearly 50 separate actuators. For large systems with dozens, hundreds, or thousands of actuation points, individual actuation is not practical and a new approach is needed.

Membrane-Driven Folding. Time- and cost-efficient folding of Soft Origami systems with hundreds or thousands of vertices requires a massively parallel, scale-robust solution not currently possible with conventional actuation. This behavior can be achieved by using elastic membranes as actuators to drive the Soft Origami folding processes. Perhaps the simplest pattern that is compatible with this folding technique, and that can serve as an instructive example, is the *accordion fold* shown in Fig. 8. The accordion fold is comprised of identical, equally spaced, repeating units. The vertices of each mountain fold remain co-planar, as do the vertices of each valley fold, so membrane-based actuation is a feasible option. The folding of this pattern would proceed in the following manner:

(1) Prestretch two membranes to suitable levels of strain (often much more than 100%) with one membrane directly above the other.
(2) Place the unfolded Soft Origami sheet between the two membranes.
(3) Bring the upper and lower membranes together.
(4) Using vacuum pressure, adhesive, or other means, fix the "valley" vertices of the Soft Origami lattice to the lower membrane, and fix the "mountain" vertices of the lattice to the upper membrane (the membranes and lattice should remain flat during this process).
(5) In a controlled manner, release the strain in the membranes while drawing them apart. The relative rates of membrane relaxation and separation will depend upon the geometry of the structure being folded. Tension between vertices must be maintained for proper constraint.

In this way, membrane-driven folding achieves simultaneous actuation and constraint of all vertices with only two actuation inputs for each membrane (to control biaxial stretching). When compared to individual actuators, a strained membrane offers a number of significant advantages:

(1) A biaxial load may be induced throughout a membrane using only two actuators; the number of *physical actuators* does not need to scale with the number of *actuation points*.
(2) Pure biaxial tension produces uniform strain in either in-plane direction of the membrane. An arbitrary "grid of dots" drawn on a membrane may be stretched or scaled as desired, mimicking uniform actuation between each of those points.
(3) Increasingly large origami patterns (increasing panel count) may be accommodated by simply increasing the size of the prestrained membranes.
(4) Relaxation of the membranes will actuate all origami points simultaneously.

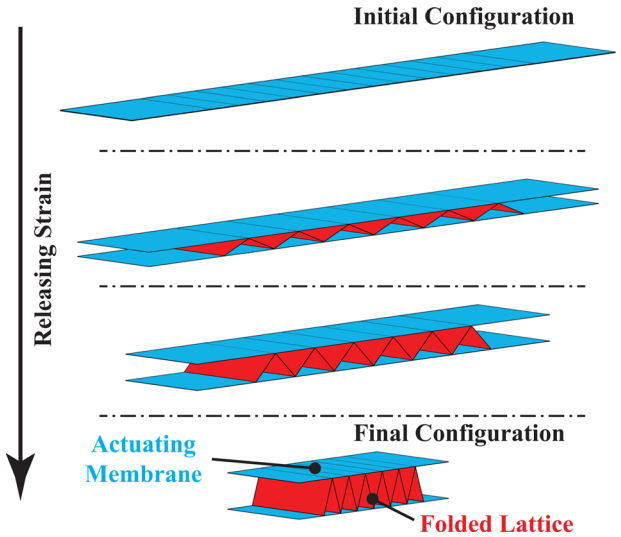

Fig. 8 Membrane-driven folding process by which a Soft Origami sheet may be folded using elastic membranes

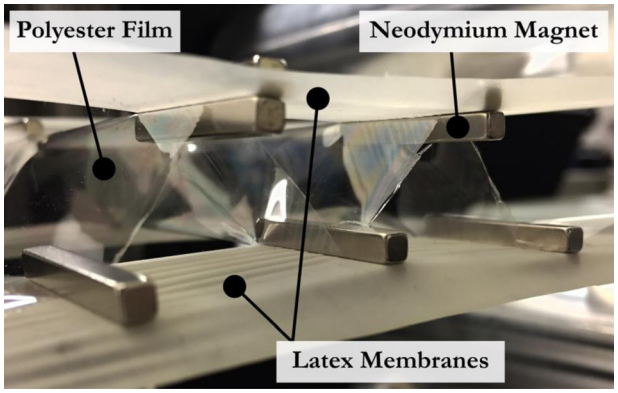

Fig. 9 Preliminary test of the membrane-driven technique. A Soft Origami polyester film is shown passing through an intermediate folding angle.

The drawback of the membrane-driven folding approach is the limited range of compatible folding patterns. A pattern is only viable for this type of folding if its prefold and postfold vertex fields are related by a linear transformation map. That is, the pre and postfold vertex fields must be related by some combination of global stretch, rotation, translation, and/or skew transformations. Membrane-driven folding sacrifices some folding complexity for the sake of scalability.

Poisson's Effect. During folding it is important to be aware of the Poisson effect within the stretched membranes, especially as the membranes actuate across a large range of strains. For an accordion fold, only one strain is released—the other must remain constant. Actuators in the nonreleased direction must be programed to correct for relaxation occurring when strain in the actuated direction is released. On a machine with only uniaxial control, the Poisson's effect may be counteracted by using a separate membrane for each row of vertices and fixing the vertices to the centers of each membrane. Although the membranes will experience the Poisson's effect, their centers (where the vertices are attached) will remain equidistant from one another. We are also investigating the use of composite membranes and membranes that have layers with tunable directional Poisson's characteristics.

Preliminary Testing. We have built and are currently testing a machine to fold Soft Origami sheets using the membrane-driven process. Figure 9 shows the result of an early test, where a two-unit Soft-Origami accordion pattern was successfully folded by the machine. In this test, polyester film (OCM ≈ 0.08) was constrained to latex membranes using neodymium magnets. The purpose of this test was to demonstrate, i.e., to show the practicality of, the folding of Soft Origami using the proposed membrane-driven technique. The regular, repeated accordion pattern and crisp folded hinges are clearly visible in Fig. 9. These are preliminary results; the design of the folding machine and comprehensive results warrant their own treatment and will be the subject of a future paper.

Conclusion

In this paper, we have introduced Soft Origami, a new class of compliant, foldable structures suitable for flexible electronics,

folding tissue scaffolds, and other applications where conventional rigid and mechanistic origami structures may not be suitable. We developed the OCM, a means by which candidate materials and geometries are evaluated for fitness within the Soft Origami regime. We demonstrate that despite their extreme compliance, Soft Origami structures can be well-constrained if held at all vertices and maintained in tension. Finally, we have introduced a scale-robust process capable of both constraining and folding Soft Origami structures, wherein just two stretching membranes are needed to drive the folding process even if the origami structure is very large.

Acknowledgment

This research was supported by the National Science Foundation and the Air Force Office of Scientific Research through the EFRI-ODISSEI program under Grant No. 1332249.

References

[1] Siegel, A. C., Phillips, S. T., Dickey, M. D., Lu, N., Suo, Z., and Whitesides, G. M., 2010, "Foldable Printed Circuit Boards on Paper Substrates," Adv. Funct. Mater., **20**(1), pp. 28–35.
[2] Chen, A. A., Thomas, D. K., Ong, L. L., Schwartz, R. E., Golub, T. R., and Bhatia, S. N., 2011, "Humanized Mice With Ectopic Artificial Liver Tissues," Proc. Natl. Acad. Sci. U.S.A., **108**(29), pp. 11842–11847.
[3] Levenberg, S., Rouwkema, J., Macdonald, M., Garfein, E. S., Kohane, D. S., Darland, D. C., Marini, R., van Blitterswijk, C. A., Mulligan, R. C., D'Amore, P. A., and Langer, R., 2005, "Engineering Vascularized Skeletal Muscle Tissue," Nat. Biotechnol., **23**(7), pp. 879–884.
[4] Stevens, K. R., Kreutziger, K. L., Dupras, S. K., Korte, F. S., Regnier, M., Muskheli, V., Nourse, M. B., Bendixen, K., Reinecke, H., and Murry, C. E., 2009, "Physiological Function and Transplantation of Scaffold-Free and Vascularized Human Cardiac Muscle Tissue," Proc. Natl. Acad. Sci. U.S.A., **106**(39), pp. 16568–16573.
[5] Glicklis, R., Merchuk, J. C., and Cohen, S., 2004, "Modeling Mass Transfer in Hepatocyte Spheroids Via Cell Viability, Spheroid Size, and Hepatocellular Functions," Biotechnol. Bioeng., **86**(6), pp. 672–680.
[6] Wood, F. M., Stoner, M. L., Fowler, B. V., and Fear, M. W., 2007, "The Use of a Non-Cultured Autologous Cell Suspension and Integra® Dermal Regeneration Template to Repair Full-Thickness Skin Wounds in a Porcine Model: A One-Step Process," Burns, **33**(6), pp. 693–700.
[7] Atala, A., Bauer, S. B., Soker, S., Yoo, J. J., and Retik, A. B., 2006, "Tissue-Engineered Autologous Bladders for Patients Needing Cystoplasty," Lancet, **367**(9518), pp. 1241–1246.
[8] Macchiarini, P., Jungebluth, P., Go, T., Asnaghi, M. A., Rees, L. E., Cogan, T. A., Dodson, A., Martorell, J., Bellini, S., Parnigotto, P. P., Dickinson, S. C., Hollander, A. P., Mantero, S., Conconi, M. T., and Birchall, M. A., 2008, "Clinical Transplantation of a Tissue-Engineered Airway," Lancet, **372**(9655), pp. 2023–2030.
[9] Shin'oka, T., Imai, Y., and Ikada, Y., 2001, "Transplantation of a Tissue-Engineered Pulmonary Artery," N. Engl. J. Med., **344**(7), pp. 532–533.
[10] Jakab, K., Norotte, C., Marga, F., Murphy, K., Vunjak-Novakovic, G., and Forgacs, G., 2010, "Tissue Engineering by Self-Assembly and Bio-Printing of Living Cells," Biofabrication, **2**(2), p. 022001.
[11] Miller, J. S., Stevens, K. R., Yang, M. T., Baker, B. M., Nguyen, D.-H. T., Cohen, D. M., Toro, E., Chen, A. A., Galie, P. A., Yu, X., Chaturvedi, R., Bhatia, S. N., and Chen, C. S., 2012, "Rapid Casting of Patterned Vascular Networks for Perfusable Engineered Three-Dimensional Tissues," Nat. Mater., **11**(9), pp. 768–774.
[12] Tachi, T., 2009, "Generalization of Rigid Foldable Quadrilateral Mesh Origami," International Association for Shell and Spatial Structures (IASS) Symposium, Valencia, Spain, Sept. 28–Oct. 2, pp. 2287–2294.
[13] Belcastro, S.-M., and Hull, T. C., 2002, "A Mathematical Model for Non-Flat Origami," Origami^3: 3rd International Meeting of Origami Mathematics, Science, and Education, Monterey, CA, Mar. 9–11, A. K. Peters, Natick, MA, pp. 39–51.
[14] Tachi, T., 2009, "Simulation of Rigid Origami," Origami, **4**, pp. 175–187.
[15] Bowen, L. A., Baxter, W. L., Magleby, S. P., and Howell, L. L., 2014, "A Position Analysis of Coupled Spherical Mechanisms Found in Action Origami," Mech. Mach. Theory, **77**, pp. 13–24.
[16] Noy, B., George, M. S., Alla, B., Nana, Y. A., and David, H. G., 2011, "Hands-Free Microscale Origami," *Origami 5*, CRC Press, Boca Raton, FL, pp. 371–384.
[17] Kuribayashi-Shigetomi, K., Onoe, H., and Takeuchi, S., 2012, "Cell Origami: Self-Folding of Three-Dimensional Cell-Laden Microstructures Driven by Cell Traction Force," PLoS One, **7**(12), p. e51085.
[18] Shenoy, V. B., and Gracias, D. H., 2012, "Self-Folding Thin-Film Materials: From Nanopolyhedra to Graphene Origami," MRS Bull., **37**(9), pp. 847–854.
[19] Liu, Y., Boyles, J. K., Genzer, J., and Dickey, M. D., 2012, "Self-Folding of Polymer Sheets Using Local Light Absorption," Soft Matter, **8**(6), pp. 1764–1769.
[20] Hawkes, E., An, B., Benbernou, N. M., Tanaka, H., Kim, S., Demaine, E. D., Rus, D., and Wood, R. J., 2010, "Programmable Matter by Folding," Proc. Natl. Acad. Sci. U.S.A., **107**(28), pp. 12441–12445.
[21] Felton, S. M., Tolley, M. T., Shin, B. H., Onal, C. D., Demaine, E. D., Rus, D., and Wood, R. J., 2013, "Self-Folding With Shape Memory Composites," Soft Matter, **9**(32), pp. 7688–7694.
[22] Ryu, J., D'Amato, M., Cui, X., Long, K. N., Qi, H. J., and Dunn, M. L., 2012, "Photo-Origami—Bending and Folding Polymers With Light," Appl. Phys. Lett., **100**(16), p. 161908.
[23] Fernandes, R., and Gracias, D. H., 2012, "Self-Folding Polymeric Containers for Encapsulation and Delivery of Drugs," Adv. Drug Delivery Rev., **64**(14), pp. 1579–1589.
[24] Bassik, N., Stern, G. M., and Gracias, D. H., 2009, "Microassembly Based on Hands Free Origami With Bidirectional Curvature," Appl. Phys. Lett., **95**(9), p. 091901.
[25] Randall, C. L., Gultepe, E., and Gracias, D. H., 2012, "Self-Folding Devices and Materials for Biomedical Applications," Trends Biotechnol., **30**(3), pp. 138–146.
[26] Timoshenko, S. P., and Goodier, J., 1951, *Theory of Elasticity*, McGraw-Hill, New York.
[27] Young, W. C., Budynas, R. G., and Sadegh, A. M., 2012, *Formulas for Stress and Strain*, 8th ed., McGraw-Hill, New York.
[28] Ashby, M. F., 2005, *Materials Selection in Mechanical Design*, Butterworth-Heinemann, Oxford, UK.
[29] Ragab, A.-R. A., and Bayoumi, S. E. A., 1998, *Engineering Solid Mechanics: Fundamentals and Applications*, CRC Press, Boca Raton, FL.